Available online at www.sciencedirect.com
SCIENCE DIRECT
Biochemical Pharmacology 68 (2004) 185–193
Biochemical Pharmacology
www.elsevier.com/locate/biochempharm

Spin adducts of several *N*-2-(2-alkoxycarbonyl-propyl)-α-pyridylnitrone derivatives with superoxide, alkyl and lipid-derived radicals

Klaus Stolze[a], Natascha Udilova[a], Thomas Rosenau[b], Andreas Hofinger[b], Hans Nohl[a,*]

[a]*Research Institute for Pharmacology and Toxicology, University of Veterinary Medicine Vienna, Veterinärplatz 1, A-1210 Vienna, Austria*
[b]*Institute of Chemistry, University of Natural Resources and Applied Life Sciences, Muthgasse 18, A-1190 Vienna, Austria*

Received 22 December 2003; accepted 16 March 2004

Abstract

Several derivatives of *N*-*t*-butyl-α-phenylnitrone (PBN) such as *N*-2-(2-ethoxycarbonyl-propyl)-α-phenylnitrone (EPPN) have recently been reported to form superoxide spin adducts ($t_{1/2}$ ca. 2–7 min at pH 7.0), which are considerably more stable than their respective PBN or DMPO adducts ($t_{1/2}$ ca. 10 and 45 s, respectively). In continuation of our studies on structure optimization of EPPN derivatives, a series of 12 novel spin traps with 2-, 3- and 4-pyridinyl substituents was synthesized and fully characterized by ^{1}H NMR, ^{13}C NMR and IR spectroscopy. In addition to the replacement of the phenyl ring by a 2-, 3- or 4-pyridinyl substituent, the ethoxy group of the parent compound EPPN was replaced by either a propoxy, *iso*-propoxy, or cyclopropylmethoxy moiety. Superoxide adducts of all PPyN derivatives were considerably more stable than those of the respective EPPN derivatives with half-lives ranging from about 6 to 11 min. In addition, alkoxyl radical adducts were also considerably more stable than those of the EPPN series. Hydroxyl radical adducts were not detected, on the other hand, very stable spin adducts were formed from a series of carbon centered radicals, e.g. from the methyl or hydroxymethyl radical. The novel spin traps are offering an alternative to PBN or POBN, especially where the higher stability of oxygen-centered radical adducts is of major importance. All of them can easily be synthesized from commercially available compounds in two or three steps.

Keywords: Spin traps; EPR; PPyN derivatives; Superoxide; Linoleic acid hydroperoxide; Free radicals

1. Introduction

The synthesis of *N*-2-(2-ethoxycarbonyl-propyl)-α-phenylnitrone (EPPN) and its derivatives has recently been described by several authors [1,2]. When compared to the structurally related spin traps PBN or POBN ($t_{1/2} \ll 1$ min [3]), the half-lives of the superoxide spin adducts of EPPN derivatives ($t_{1/2}$ = 2–7 min [1,2]) are similar to the recently reported values for the spin traps EMPO ($t_{1/2}$ = 8.6 min [4–7]) or Trazon ($t_{1/2}$ = 3.6 min [8,9]), but lower than the respective number for DEPMPO ($t_{1/2}$ = 14.8 min [10,11]). Since the latter compound bears strongly electron-withdrawing groups, it was expected that the incorporation of an additional electron acceptor substituent into the molecule of EPPN derivatives might lead to an increased stability of the superoxide adducts. Furthermore, the possibility to obtain a series of compounds with different lipophilicity will facilitate the investigation of radicals in lipid membranes. In this respect, the detection of free radicals from lipid peroxidation has already been investigated using different spin traps, such as DMPO [12], DEPMPO [11,13], EMPO [6] or Trazon [9], but an optimal spin trap for the detection of alkoxyl radicals has not yet been found.

It was thus the aim of the present study to evaluate the effect of the introduction of a pyridinyl ring (2-, 3- and

Abbreviations: DEPMPO, 5-(diethoxyphosphoryl)-5-methyl-1-pyrroline *N*-oxide; DMPO, 5,5-dimethylpyrroline *N*-oxide; DTPA, diethylenetriaminepentaacetic acid; EMPO, 5-(ethoxycarbonyl)-5-methyl-1-pyrroline *N*-oxide; EPPN, *N*-2-(2-ethoxycarbonyl-propyl)-α-phenylnitrone; EPPyN-2, *N*-2-(2-ethoxycarbonyl-propyl)-α-(2-pyridinyl)nitrone; EPPyN-3, *N*-2-(2-ethoxycarbonyl-propyl)-α-(3-pyridinyl)nitrone; EPPyN-4, *N*-2-(2-ethoxycarbonyl-propyl)-α-(4-pyridinyl)nitrone; EPR, electron paramagnetic resonance; HFS, hyperfine splitting; LO•, lipoxyl radical; NMR, nuclear magnetic resonance; $O_2^{\bullet -}$, superoxide anion radical; PBN, *N*-*tert*-butyl-α-phenylnitrone; POBN, α-(4-pyridinyl-1-oxide)-*N*-*tert*-butylnitrone; SOD, superoxide dismutase; Trazon, 1,3,3-trimethyl-6-azabicyclo[3.2.1]oct-6-ene-*N*-oxide

* Corresponding author. Tel.: +43-1-25077-4400; fax: +43-1-25077-4490.
E-mail address: hans.nohl@vu-wien.ac.at (H. Nohl).

0006-2952/$ – see front matter © 2004 Elsevier Inc. All rights reserved.
doi:10.1016/j.bcp.2004.03.017

4-pyridinyl derivatives) as well as the alteration of the alkoxy group in the ester moiety of the PPyN derivatives on the stability of the radical adducts, especially with regard to the stability of oxygen-centered radicals, such as superoxide, hydroxyl or alkoxyl radicals.

2. Materials and methods

2.1. Chemicals

2-Bromo-2-methylpropionyl bromide, linoleic acid, superoxide dismutase and xanthine oxidase were commercially available from Sigma–Aldrich. Petroleum ether (high boiling, 50–70 °C) was obtained from Fluka, all other chemicals from Merck.

2.2. Syntheses

Synthesis and characterization of the compounds were performed as reported earlier [2], analogous to the synthesis of EMPO and its derivatives [4–7] with minor adaptations as given below.

2.2.1. Alkyl 2-bromo-2-methylpropionate

2-Bromo-2-methylpropionyl bromide (70 mmol) was slowly added to a solution of the respective alcohol (100 mmol) and pyridine (70 mmol) in chloroform at 0 °C (ice bath). After stirring for 1 h, the reaction mixture was successively washed with water (50 ml), sulfuric acid (10%, 50 ml) and concentrated aqueous sodium bicarbonate (50 ml), and dried over Na_2SO_4 overnight. Solvent and excess alcohol were removed under reduced pressure. The crude, nearly colorless product was used without further purification.

2.2.2. Alkyl 2-methyl-2-nitropropionate

The respective alkyl 2-bromo-2-methylpropionate (60 mmol) was added under stirring to a solution of sodium nitrite (7.2 g, 104 mmol) and phloroglucinol dihydrate (8.5 g, 52 mmol) in dry *N*,*N*-dimethylformamide (120 ml) at room temperature. The solution was stirred for 3 days, poured into ice water (240 ml), and extracted four times with ethyl acetate (100 ml). The combined extracts were treated twice with 100 ml of saturated sodium bicarbonate solution and dried over Na_2SO_4. After removal of the solids by filtration, the solvent was evaporated in vacuo. The obtained colorless or pale yellow products were used further without purification.

2.2.3. Synthesis of nitrones

To a concentrated solution of the respective alkyl 2-methyl-2-nitropropionate (25 mmol) in H_2O/CH_3OH (v/v = 6:4) the respective aldehyde (30 mmol of either 2-, 3-, 4-pyridine carbaldehyde or benzaldehyde) and aqueous ammonium chloride solution (1.87 g in 8 ml of water) were added. The mixture was carefully kept at room temperature, while 3.27 g (50 mmol) of zinc dust was slowly added within 30 min. After stirring for 4.5 h at room temperature, the white precipitate and the remaining zinc powder was removed by filtration, and the solid residue was washed five times with 30 ml of methanol. The combined liquid phases were concentrated to a volume of about 10 ml, saturated with borax and extracted four times with 60 ml of dichloromethane. The combined extracts were dried over Na_2SO_4, filtered, and concentrated. Column chromatography on silica gel (petroleum ether/ethanol (1–5%) with gradient elution) afforded 20–30% (overall yield) of a light-brown product, which was recrystallized from pentane and characterized by ^{1}H NMR, ^{13}C NMR, and IR spectroscopy (see Tables 1–3).

Table 1
^{13}C NMR data (ppm) of the spin traps

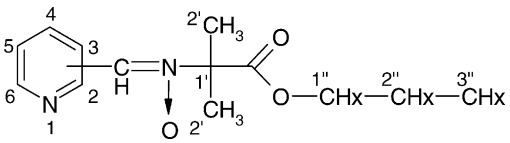

	^{1}Ar	^{2}Ar	^{3}Ar	^{4}Ar	^{5}Ar	^{6}Ar	CH	$^{1'}$C	$^{2'}$C	COO	$^{1''}$C	$^{2''}$C	$^{3''}$C
EPPyN2	(N)	149.87	124.8	137.3	124.4	149.92	133.1	78.2	24.8	170.5	62.5	14.3	–
EPPyN3	(N)	150.6	127.3	135.1	123.9	151.1	128.7	77.9	24.8	170.5	62.6	14.3	–
EPPyN4	(N)	149.7	121.8	137.3	121.8	149.7	129.0	78.3	24.4	169.9	62.3	13.9	–
PPPyN2	(N)	149.47	124.3	136.9	123.9	149.42	132.6	77.8	24.4	170.1	67.5	21.7	10.1
PPPyN3	(N)	150.6	127.4	135.3	123.9	151.0	128.7	78.0	24.8	170.6	68.1	22.2	10.6
PPPyN4	(N)	150.8	122.1	137.2	122.1	150.8	129.6	78.7	24.8	170.4	68.2	22.2	10.6
iPPPyN2	(N)	149.57	124.3	136.8	123.9	149.41	132.6	77.7	24.3	169.6	69.8	21.1	–
iPPPyN3	(N)	150.0	126.9	134.8	123.4	150.5	128.2	77.4	24.3	169.6	69.8	21.4	–
iPPPyN4	(N)	149.4	120.7	135.9	120.7	149.4	128.2	77.2	23.6	169.0	69.1	20.4	–
CPPyN2	(N)	149.45	124.4	136.8	124.0	149.38	132.7	77.8	24.4	170.2	70.7	9.5	3.1
CPPyN3	(N)	150.0	127.0	134.9	123.5	150.5	128.4	77.6	24.4	170.3	70.8	9.5	3.1
CPPyN4	(N)	150.3	121.6	136.8	121.6	150.3	129.3	78.3	24.4	170.1	70.8	9.5	3.1
CPPN	130.4	128.4	128.9	130.5	128.9	128.4	131.2	77.1	24.5	170.6	70.6	9.6	3.1
EPPN	130.4	129.1	128.6	130.7	128.6	129.1	131.3	77.1	24.5	170.6	62.1	14.0	–

Table 2
^{1}H NMR data (ppm) of the spin traps

	^{1}ArH	^{2}ArH	^{3}ArH	^{4}ArH	^{5}ArH	^{6}ArH	HC=N	$^{2'}CH_3$	OCH_x	$^{2''}CH_x$	$^{3''}CH_x$
EPPyN2	(N)	–	8.61d	7.28m	7.76td	9.15d	7.82s	1.84s	4.25q	1.26t	–
EPPyN3	(N)	8.97s	–	8.59d	7.36t	9.06d	7.58s	1.85s	4.26q	1.30t	–
EPPyN4	(N)	8.69d	8.09d	–	8.09d	8.69d	7.55s	1.84s	4.26q	1.28t	–
PPPyN2	(N)	–	8.62d	7.29m	7.80td	9.15d	7.86s	1.86s	4.18t	1.68m	0.95t
PPPyN3	(N)	8.98s	–	8.59d	7.35t	9.05d	7.55s	1.81s	4.16t	1.67m	0.92t
PPPyN4	(N)	8.62d	8.05d	–	8.05d	8.62d	7.51s	1.81s	4.14q	1.68m	0.90t
iPPPyN2	(N)	–	8.63d	7.29m	7.78td	9.16d	7.82s	1.82s	5.09spt	1.26d	–
iPPPyN3	(N)	8.97s	–	8.57d	7.34t	9.03d	7.58s	1.85s	5.08spt	1.23d	–
iPPPyN4	(N)	8.68d	8.04d	–	8.04d	8.68d	7.52s	1.84s	5.09spt	1.26d	–
CPPyN2	(N)	–	8.65d	7.30m	7.79td	9.18d	7.86s	1.86s	4.05d	1.14m	0.53m/0.29m
CPPyN3	(N)	8.99s	–	8.61d	7.38t	9.08d	7.56s	1.85s	4.26d	1.15m	0.55m/0.30m
CPPyN4	(N)	8.69d	8.05d	–	8.05d	8.69d	7.53s	1.85s	4.05d	1.14m	0.55m/0.29m
CPPN	–	8.27m	7.42m	7.42m	7.42m	8.27m	7.48s	1.84s	4.05d	1.15m	0.52m/0.27m
EPPN	–	8.28m	7.42m	7.42m	7.42m	8.28m	7.49s	1.82s	4.25q	1.27t	

s, singlet; d, doublet; t, triplet; q, quadruplet; spt, septet; m, multiplet; td, triplet of doublets.

The purity of the products was assessed by TLC and UV spectroscopy.

2.2.4. Preparation of lipid hydroperoxides

Linoleic acid hydroperoxide was synthesized according to O'Brien [14]. Briefly, linoleic acid was air-oxidized for 72 h in the dark at room temperature. The oxidation mixture was dissolved in petroleum ether (boiling range 60–90 °C) and extracted four times with water/methanol (v/v = 1:3). The obtained methanolic phase was counter-extracted four times with petroleum ether (boiling range 60–90 °C) and evaporated under reduced pressure. The obtained hydroperoxide was dissolved in ethanol and stored in liquid nitrogen. The concentration of hydroperoxide was determined by UC spectroscopy based on an extinction coefficient of $\varepsilon_{233nm} = 25{,}250\ M^{-1}\ cm^{-1}$ in ethanol [14].

2.3. Instruments

UV-Vis spectra were recorded on Hitachi 150-20 and U-3300 spectrophotometers in double-beam mode against a blank of the respective solvent. Determination of the concentrations was done measuring the absorption maxima in the range between 200 and 350 nm.

IR spectra were recorded as film on an ATI Mattson Genesis Series FTIR spectrometer (see also Table 3).

For EPR experiments the Bruker spectrometer ESP300E was used, operating at 9.7 GHz with 100 kHz modulation frequency, equipped with a rectangular TE_{102} or a TM_{110} microwave cavity.

^{1}H NMR spectra were recorded at 300 MHz, ^{13}C NMR spectra at 75.47 MHz on a Bruker Avance. $CDCl_3$ containing tetramethylsilane (TMS) as the internal standard was used as the solvent throughout. ^{13}C peaks were assigned by means of attached proton test (APT), ^{1}H-detected heteronuclear multiple-quantum coherence (HMQC) and heteronuclear multiple bond connectivity (HMBC) spectra. A complete set of ^{1}H, H–H correlated, ^{13}C, HMQC and HMBC spectra was recorded for each compound. All chemical shift data are given in ppm units.

3. Results

3.1. Structure of the spin traps

The identity of the synthesized spin traps was unambiguously proven by NMR. In the ^{1}H NMR spectra, the typical pattern of differently substituted pyridines was produced. In general, the electron-deficient character of the aromatic pyridine system became evident by a significant down-field shift of the resonances: in comparison to benzene as the standard aromatic system (7.28 ppm) the pyridine resonances appear between 7.3 and 9.2 ppm according to the respective substitution pattern. The signals with the largest downfield shift originate from the protons 2 and 6 neighboring the electronegative pyridine nitrogen. The 2-substituted aromatic gave a typical higher-order pattern consisting of two duplets (H-3 and H-6) and two multiplets (H-4 and H-5). The 3-substituted pyridine ring showed a prominent singlet for H-2 and two duplets and a triplet for H-4, H-6, and H-5, respectively. In the 4-substituted derivatives with their additional mirror symmetry, H-2/H-6 and H-3/H-5 become magnetically equivalent resulting in two duplets of double intensity.

The benzylidenic proton appeared throughout as a singlet without long-range couplings. Also here, the influence of the electronegative nitrogen with its electron-acceptor properties was noticeable. Increasing proximity of the pyridine nitrogen causes a down-field shift: the resonances of the PPyN-2 derivatives appear at about 7.82 ppm, those of the PPyN-3 species at about 7.58 ppm, and those of the PPyN-4 compounds at 7.52 ppm.

The resonance of the two magnetically equivalent 2′-methyl groups is found at about 1.85 ppm throughout. In general, the influence of the alkoxy moiety on the NMR

Table 3
IR data (cm^{-1}) of the spin traps

EPPyN2	3102	3053	**2986**	2940	**1746**	–	**1563**	**1456**	**1436**	**1398**	–	**1364**	**1275**	**1178**	**1155**	**1118**	1089	**1025**	988	910	859	817	763	740	698
EPPyN3	3088	3048	2985	2941	**1744**	1576	**1559**	1471	1418	1406	1387	1365	**1284**	**1177**	**1156**	**1130**	1096	1024	–	908	859	824	762	**706**	–
EPPyN4[a]	3085	3035	2983	2939	**1742**	**1593**	**1571**	1469	1445	**1416**	1389	**1365**	**1281**	**1177**	**1156**	**1133**	–	1024	989	910	–	**839**	794	762	695
PPPyN2	3054	–	**2969**	2940	**1746**	–	**1563**	**1456**	**1436**	**1398**	–	**1364**	**1283**	**1175**	**1148**	**1119**	1089	1047	988	967	903	817	764	740	698
PPPyN3	3079	–	**2967**	2937	**1743**	**1578**	**1562**	1471	**1420**	**1406**	**1390**	1364	**1287**	**1269**	**1161**	**1152**	**1114**	**1094**1051	1023	960	891	856	809		**707**
PPPyN4	3090	3042	2967	2940	**1745**	**1593**	**1574**	1540	1472	**1420**	1391	1365	**1286**	**1162**	**1132**	1090	1053	–	989	965	892	**851**	801	755	694
iPPPyN2	–	3052	**2982**	2940	**1742**	**1563**	1470	**1456**	**1436**	**1398**	**1387**	**1364**	**1283**	**1177**	**1119**	**1105**	1047	988	961	920	901	**817**	764	740	697
iPPPyN3	3161	3078	2982	2940	**1742**	1577	**1561**	1468	**1421**	1387	1365	–	**1284**	**1168**	**1128**	**1104**	–	**1025**	**1005**	961	900	825	–	**706**	–
iPPPyN4	3148	3038	2982	2940	**1742**	**1594**	**1572**	1470	**1417**	1388	1366	**1282**	1206	**1176**	**1133**	**1104**	–	–	989	962	902	**840**	762	–	694
CPPyN2	3084	3052	2995	2948	**1744**	–	**1562**	**1456**	**1436**	**1398**	**1364**	–	**1283**	**1158**	**1119**	1089	1047	1024	972	894	–	817	763	739	697
CPPyN3	3084	–	2993	2949	**1739**	1575	1558	1463	1417	1388	1365	**1284**	**1267**	**1157**	**1123**	–	–	1023	969	892	–	826	760	**705**	–
CPPyN4	3087	–	2998	2948	**1743**	**1594**	**1572**	1463	**1416**	1389	1366	**1282**	1206	**1159**	**1133**	–	–	1023	989	972	895	838761	–		696
CPPN	3082	3005	2991	2948	**1742**	**1582**	1566	1473	**1446**	1417	1385	1365	**1280**	**1155**	–	**1112**	1077	1022	974	–	–	890	–	757	**693**
EPPN[a]	3091	3058	2985	2939	**1742**	**1580**	1563	**1469**	**1446**	**1413**	**1387**	**1364**	**1280**	**1177**	**1154**	**1119**	–	**1025**	–	906	–	859	808	755	**693**

Intensities: strong (**1746**), medium (**1563**), weak (988).
[a] Data from Stolze et al. [2].

shifts of the acid part is generally rather low, so that—as intended—the variation of the alkoxy part did indeed influence solubility and lipophilicity properties, but did not alter the stability of the spin adducts. The cyclopropyl protons of the cyclopropylmethoxy moiety showed the expected upfield shift with resonances at 1.15, 0.50, and 0.30 ppm.

The ^{13}C NMR data were very consistent. In N–O derivatives with a C=N double bond, such as oximes, nitroxides or nitrones, the *Z*-configured α-C atoms are characteristically shifted upfield by 6–10 ppm [15]. With an expected resonance at about 135–140 ppm, the chemical shift of the benzylidenic carbon at 128 ppm is indicative of its *Z*-arrangement with regard to the oxygen. Thus, only the isomers with the C=N double bond in *E*-configuration were formed in the synthesis, so that the sterically demanding substituents, i.e. the pyridine ring and the alkyl ester moiety, are placed *trans*. Also in the ^{13}C NMR spectra the electron-deficient nature of the pyridine moiety was reflected. While the aromatic resonances in EPPN derivatives were found between 128 and 130 ppm, the resonances of the pyridine rings in the different PPyN derivatives experienced significant changes: a very strong downfield shift for C-2 and C-6, which neighbor the nitrogen (150 ppm), a weak downfield shift for C-3 and C-5 at about 124 ppm and an upfield shift for C-4 at about 134 ppm. The nitrone substituent causes a slight downfield shift in *ipso* position by 2–3 ppm and a very weak up-field effect at the neighboring carbon atoms (<1 ppm).

In analogy to the ^{1}H spectra, also the ^{13}C results proved that changes in the alkoxy part of the ester moieties remained without significant influences on the resonances of the nitrone. C-1′ appeared generally at about 78 ppm, C-2′ at 24.5 ppm and the carboxyl carbon at 169–170 ppm. The respective NMR data are summarized in Tables 1 and 2.

3.2. Spin trapping of superoxide radicals

In Fig. 1 the general structure of the spin traps is shown. In Fig. 2a, the EPR spectrum of the superoxide adduct of iPPPyN-2 (20 mM) is given as an example. The adduct was generated in the xanthine/xanthine oxidase system at pH 7.4. No EPR spectrum was observed in the presence of SOD (Fig. 2b). Under these conditions similar spectra were obtained from EPPyN-4 in the absence (Fig. 2c) or presence of SOD (Fig. 2d). From CPPN (Fig. 2e) however, an intensive and well-resolved spectrum could only obtained using an incubation system with solid KO_2. This system was also used in order to determine the half-life of superoxide adducts: the respective spin traps (20 mM, final concentration) were incubated in water/DMSO in the presence of ca. 0.5 mg solid KO_2 for 15 s, after which phosphate buffer (300 mM, final pH 7.0) containing 20 mM DTPA, SOD (100 U/mL), catalase (250 U/mL) and 5% DMSO was added. A series of consecutive spectra was recorded until the superoxide-related lines gradually disappeared (after about 15–20 min) and additional lines of lower intensity,

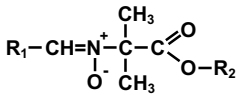

EPPyN2:	**R_1 = 2-Pyridinyl**
	R_2 = C_2H_5
EPPyN3:	**R_1 = 3-Pyridinyl**
	R_2 = C_2H_5
EPPyN4:	**R_1 = 4-Pyridinyl**
	R_2 = C_2H_5
PPPyN2:	**R_1 = 2-Pyridinyl**
	R_2 = C_3H_7
PPPyN3:	**R_1 = 3-Pyridinyl**
	R_2 = C_3H_7
PPPyN4:	**R_1 = 4-Pyridinyl**
	R_2 = C_3H_7
iPPPyN2:	**R_1 = 2-Pyridinyl**
	R_2 = *iso*-C_3H_7
iPPPyN3:	**R_1 = 3-Pyridinyl**
	R_2 = *iso*-C_3H_7
iPPPyN4:	**R_1 = 4-Pyridinyl**
	R_2 = *iso*-C_3H_7
CPPyN2:	**R_1 = 2-Pyridinyl**
	R_2 = *cyclo*-C_3H_5-CH_2
CPPyN3:	**R_1 = 3-Pyridinyl**
	R_2 = *cyclo*-C_3H_5-CH_2
CPPyN4:	**R_1 = 4-Pyridinyl**
	R_2 = *cyclo*-C_3H_5-CH_2
CPPN:	**R_1 = Phenyl**
	R_2 = *cyclo*-C_3H_5-CH_2

Fig. 1. General structure of the spin traps.

coming from a carbon-centered degradation product, became predominant. The contribution of these secondary lines was then subtracted from each individual EPR spectrum before calculating the respective half-life. The resulting intensity decrease of the first two lines was approximated by a first-order exponential decay. This kind of approximation was in a good agreement with the experimental data. The Pearson correlation coefficient, which characterizes the certainty of approximation, was higher than 0.99 for all spin traps investigated, except for CPPN and CPPyN-2, where these values were 0.97 and 0.98, respectively. The respective values of apparent superoxide half-lives are listed in Table 4. The obtainable spectral intensity (measured after 5 min incubation with the xanthine/xanthine oxidase system) was higher compared with DMPO, but lower than with DEPMPO, decreasing from the hydrophilic to the lipophilic compounds due to increasing steric hindrance.

3.3. Spin adduct formation with oxygen-containing radicals

No hydroxyl radical adducts were detected in a Fenton system in the presence of any of the investigated spin traps.

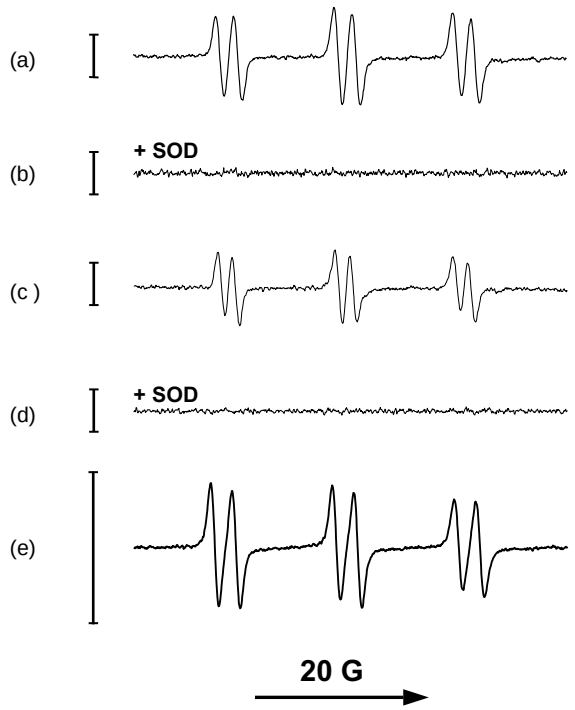

Fig. 2. Formation of the superoxide adducts of the spin traps iPPPyN-2, EPPyN-4 and CPPN. (a) iPPPyN-2 (20 mM), catalase (250 U/mL), xanthine (0.2 mM) and xanthine oxidase (50 mU/mL) in oxygenated phosphate buffered saline (20 mM, pH 7.4, containing 0.4 mM DTPA and 5% DMSO) were incubated and measured using the following EPR parameters: sweep width, 50 G; modulation amplitude, 1 G; microwave power, 20 mW; time constant, 0.16 s; receiver gain, 2×10^5; scan rate, 35.8 G/min. The bars represent 10,000 arbitrary units. (b) Same as in (a), except that SOD (100 U/ml) was added. (c) Same as in (a), except that EPPyN-4 (20 mM) was used. EPR parameters: sweep width, 50 G; modulation amplitude, 1 G; microwave power, 20 mW; time constant, 0.16 s; receiver gain, 2×10^5; scan rate, 35.8 G/min. (d) Same as in (c), except that SOD (100 U/ml) was added. (e) CPPN (20 mM in H_2O containing 10% DMSO) was incubated for 10 s with 0.5 mg solid KO_2 and then diluted 1:1 with phosphate buffer (300 mM, pH 7, containing 20 mM DTPA). EPR parameters: sweep width, 50 G; modulation amplitude, 1 G; microwave power, 20 mW; time constant, 0.04 s; receiver gain, 2×10^5; scan rate, 143.1 G/min.

Table 4
Half-life of the superoxide adducts and *n*-octanol/buffer partition coefficients of the spin traps

Compound	Apparent $t_{1/2}$ (min)	Partition coefficient *n*-octanol/phosphate buffer (100 mM, pH 7.4)
EPPyN-2	5.79	7.2
EPPyN-3	10.68	2.4
EPPyN-4	7.28[a]	3.7[a]
PPPyN-2	4.61	23.2
PPPyN-3	10.07	7.9
PPPyN-4	6.14	12.7
iPPPyN-2	7.54	25.1
iPPPyN-3	9.60	5.5
iPPPyN-4	6.49	8.2
CPPyN-2	8.50	19.4
CPPyN-3	10.20	10.0
CPPyN-4	6.40	11.9
CPPN	4.13	72.6

[a] Data from Stolze et al. [2].

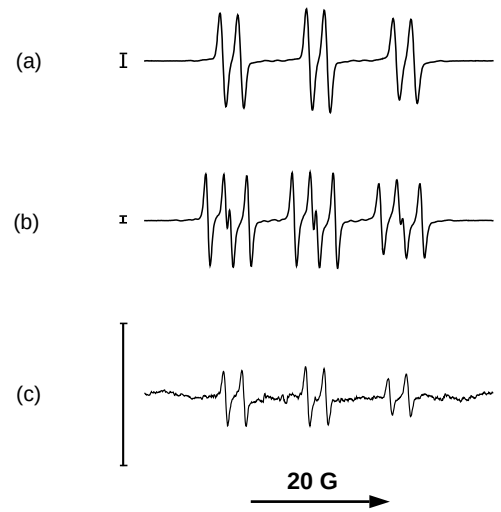

Fig. 3. Iron-dependent formation of two different EPPyN-4 spin adducts from methanol (a) EPPyN-4 (20 mM) was incubated with a Fenton system containing 10% methanol, $FeSO_4$ (1 mM), EDTA (2 mM), H_2O_2 (0.2%) and the reaction was stopped after 10 s by 1:1 dilution with phosphate buffer (300 mM, pH 7.4, containing 20 mM DTPA) and the spectrum was recorded using the following spectrometer settings: sweep width, 60 G; modulation amplitude, 0.24 G; microwave power, 20 mW; time constant, 0.08 s; receiver gain, 1×10^4; scan rate, 42.9 G/min. The bars represent 10,000 arbitrary units. (b) Same conditions, except that methanol-^{13}C-d_3 was used. (c) After a 10 s incubation of EPPyN-4 (1 M in methanol) with $FeCl_3$ (10 mM), the reaction was stopped by 1:20 dilution with phosphate buffer (0.15 M, pH 7.4, containing 10 mM DTPA), and the spectrum was recorded with the following spectrometer settings: sweep width, 60 G; modulation amplitude, 0.68 G; microwave power, 20 mW; time constant, 0.08 s; receiver gain, 1×10^4; scan rate, 42.9 G/min.

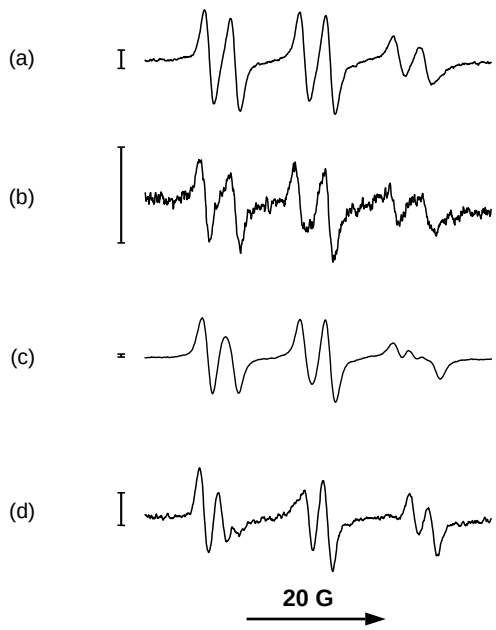

Fig. 4. Iron-dependent formation of spin adducts from *n*-octanol and the spin traps iPPPyN-2 and iPPPyN-3. (a) After a 10 s incubation of iPPPyN-2 (1 M in *n*-octanol) with $FeCl_3$ (10 mM), the reaction was stopped by 1:20 dilution with phosphate buffer (0.15 M, pH 7.4, containing 10 mM DTPA), and the spectrum was recorded with the following spectrometer settings: sweep width, 50 G; modulation amplitude, 1 G; microwave power, 20 mW; time constant, 0.33 s; receiver gain, 4×10^5; scan rate, 35.8 G/min. The bars represent 10,000 arbitrary units. (b) Same conditions, except that iPPPyN-3 was used. (c) Same as (a), secondary product formed after 42 min. (d) Same as (b), secondary product formed after 33 min.

However, within a few minutes the EPR spectrum of a secondary product gradually appeared, with parameters being typical of a carbon-centered radical adduct (Table 5, spectrum not shown). After prolonged incubation, other secondary species, such as the respective (2-alkoxy-carbonyl-propyl)-2-aminoxyl [1,2] were also detected.

In the presence of methanol and iron, two different radical adducts were found. A Fenton system in the presence of 5% methanol according to Roubaud et al. [1] resulted in the formation of the respective hydroxymethyl radical adduct, as shown in Fig. 3a for the EPPyN-4/$^{\bullet}CH_2OH$ species. The identification as a carbon-centered radical adduct was possible by using ^{13}C-labeled methanol (Fig. 3b), where an additional carbon splitting became visible.

In Fig. 3c the EPR spectrum of the methoxyl radical adduct of EPPyN-4 is shown, which was obtained after nucleophilic addition of methanol to EPPyN-4 in the presence of Fe^{3+} under the experimental conditions reported by Dikalov and Mason [12], except that the incubation time was reduced to 10 s in order to suppress the formation of secondary products. The observed HFS values ($a^N = 14.05$ G; $a^H = 3.03$ G) are clearly different from those of the hydroxymethyl radical adduct obtained in the above-mentioned Fenton system containing 5% methanol ($a^N = 14.92$ G; $a^H = 3.09$ G). In addition, the use of ^{13}C-labeled methanol did not result in an additional splitting. The data of radical adducts obtained from the other spin traps under study are listed in Table 5.

This set of experiments was repeated with higher alcohols such as ethanol or *n*-octanol. With increasing chain length the formation of the respective oxygen centered radical adducts became more and more difficult. The *n*-octyloxyl adduct was only obtained as a rather short-lived species from the spin traps iPPPyN-2 (Fig. 4a) and iPPPyN-3 (Fig. 4b). In both cases, the original EPR spectra faded after several minutes, and signals of secondary carbon-centered radical adducts from iPPPyN-2 and iPPPyN-3 appeared (Fig. 4c and d, respectively). The asymmetric lines observed with adducts from asymmetric radicals (e.g. from the α-hydroxyethyl radical) are most probably due to the formation of different stereoisomers (diastereomers and conformers) with HSF splitting differences being comparable to the line width. In those cases where the line asymmetry was big enough, the spectral contribution of the two individual stereoisomers was assessed by computer simulation (see Table 5).

3.4. Spin trapping of lipid-derived free radicals

We also investigated the detection of radicals derived from linoleic acid by lipid peroxidation-type processes. An

Table 5
Comparison of the EPR parameters of different radical adducts of various PPyN derivatives

Radical HFS (G)		EPPyN-2	EPPyN-3	EPPyN-4	PPPyN-2	PPPyN-3	PPPyN-4	iPPPyN-2[a]	iPPPyN-3[a]	iPPPyN-4[a]	CPPyN-2	CPPyN-3	CPPyN-4	CPPN
•OOH	a^N	13.85	13.85	13.67[b]	13.83	13.85	13.69	13.77	13.83	13.67	13.81	13.82	13.67	14.16
	a^H	2.03	1.68	1.60	2.07	1.65	1.66	2.05	1.67	1.64	2.12	1.67	1.67	2.45
•C(•OH)	a^N	15.05	15.26	14.67[b]	15.04	15.23	15.03	15.00	15.17	15.02	15.06	15.30	15.05	15.44
	a^H	3.51	2.81	3.43	3.51	2.83	3.08	3.52	2.77	2.92	3.59	2.98	3.15	3.84
•H	a^N	15.78	15.90	15.65[b]	15.75	15.90	15.60	15.72	15.86	15.63	15.73	15.89	15.64	16.05
	$a^{H(2)}$	10.30	10.56	9.99	10.28	10.56	9.93	10.33	10.60	9.99	10.33	10.73	10.04	10.60
•CH_3	a^N	15.41	15.53	14.66[b]	15.39	15.51	15.35	15.35	15.50	15.33	15.38	15.52	15.34	15.69
	a^H	3.91	2.95	3.43	3.99	3.00	3.27	3.88	2.98	3.20	3.90	2.95	3.20	3.92
•OCH_3	a^N	14.30	14.31	14.05[b]	14.34	14.30	14.16	14.20	14.27	14.12	14.25	14.26	14.10	14.56
	a^H	3.60	3.20	3.03	3.61	3.15	3.23	3.58	3.16	3.16	3.80	3.35	3.17	4.33
•CH_2OH	a^N	14.98	15.11	14.92[b]	14.95	15.10	14.94	14.87	15.04	14.89	14.93	15.07	14.90	15.26
	a^H	3.58	2.83	3.09	3.59	2.83	3.08	3.52	2.81	3.06	3.57	2.85	3.09	3.86
•OC_2H_5	a^N	14.39	14.42	14.27	14.40	14.40	14.30	14.29	14.34	14.20	14.30	14.36	14.24	14.64
	a^H	4.01	3.60	3.56	3.96	3.60	3.60	3.91	3.53	3.43	4.10	3.80	3.72	4.62
•$CH(OH)CH_3$	a^N	15.08	15.21	14.99	15.04	15.17	15.01	14.96	15.13	14.97	15.03	15.16	14.99	15.38
	a^H	3.81 (47%)	3.03 (50%)	3.08 (50%)	3.86 (47%)	3.03 (50%)	3.20 (50%)	3.85 (47%)	3.00 (50%)	3.17 (50%)	4.00 (47%)	3.10 (50%)	3.28 (50%)	3.71 (50%)
	a^H	2.31 (53%)	2.01 (50%)	2.19 (50%)	2.36 (53%)	2.03 (50%)	2.20 (50%)	2.39 (53%)	2.00 (50%)	2.17 (50%)	2.52 (53%)	2.10 (50%)	2.28 (50%)	3.01 (50%)
•OC_8H_{17}	a^N	–	–	–	–	–	–	13.75	13.75	–	–	–	–	–
	a^H	–	–	–	–	–	–	3.75	4.40	–	–	–	–	–
•$C(CH_3)_2OH$	a^N	15.05	15.19	14.97	15.04	15.17	15.01	14.95	15.11	14.98	15.02	15.15	15.00	15.37
	a^H	3.96	3.14	3.13	3.92	3.16	2.17	3.93	3.13	2.19	4.06	3.21	3.33	3.05
	a^H	2.36 (50%)	2.04 (50%)	2.13 (50%)	2.28 (50%)	2.00 (50%)	3.17 (50%)	2.33 (50%)	2.03 (50%)	3.19 (50%)	2.46 (50%)	2.11 (50%)	2.23 (50%)	4.05 (50%)
•CO_2^-	a^N	15.01	15.08	14.95[b]	14.98	15.05	14.90	14.92	15.04	14.89	14.97	15.04	14.90	15.16
	a^H	3.30	3.64	3.49	3.31	3.65	3.44	3.23	3.66	3.45	3.33	3.82	3.54	4.62
•C(LOOH)	a^N	14.81	14.94	15.02	14.86	15.17	14.73	14.60	14.88	14.71	14.66	15.03	14.74	15.48
	a^H	3.18 (60%)	2.60 (40%)	2.75 (40%)	3.23 (60%)	2.49 (40%)	2.82 (40%)	3.11 (40%)	2.52 (40%)	2.78 (40%)	3.23 (40%)	2.63 (40%)	2.87 (40%)	2.95 (50%)
	a^N	15.62	15.50	15.42	15.66	15.55	15.39	15.30	15.44	15.31	15.36	15.41	15.30	15.48
	a^H	3.11 (40%)	2.54 (60%)	2.67 (60%)	3.15 (40%)	2.43 (60%)	2.74 (60%)	3.19 (60%)	2.52 (60%)	2.74 (60%)	3.15 (60%)	2.57 (60%)	2.79 (60%)	3.95 (50%)
Best fit for single species	a^N	15.13	15.28	15.26	15.18	15.40	15.13	15.02	15.22	15.07	15.08	15.26	15.08	15.48
	a^H	3.15	2.56	2.69	3.20	2.45	2.77	3.16	2.52	2.76	3.18	2.59	2.82	3.45

[a] Slow degradation (loss of isopropyl group).
[b] Data from Stolze et al. [2].

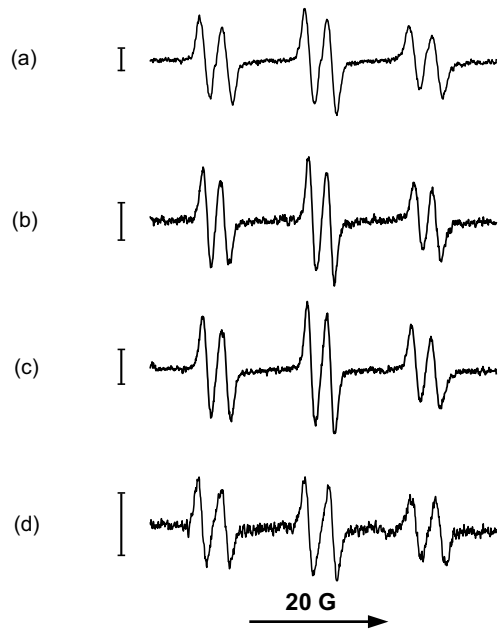

Fig. 5. Detection of a lipid-derived radical adduct from peroxidized linoleic acid using a Fenton-type incubation system in the presence of the spin traps CPPyN-2, CPPyN-3, CPPyN-4 and CPPN. (a) To a nitrogen-bubbled solution of peroxidized linoleic acid (2 mM) and CPPyN-2 (20 mM) in phosphate buffer (20 mM, pH 7.4, containing 1.5% acetonitrile) $FeSO_4$ (0.2 mM) was added and the spectrum was recorded with the following spectrometer settings: sweep width, 50 G; modulation amplitude, 0.3 G; microwave power, 20 mW; time constant, 0.16 s; receiver gain, 2×10^5; scan rate, 17.9 G/min. The bars represent 10,000 arbitrary units. (b) Same conditions, except that CPPyN-3 was used. (c) Same conditions, except that CPPyN-4 was used. (d) Same conditions, except that CPPN was used.

anaerobic setup, obtained by flushing with nitrogen for several minutes, was chosen. The reaction system consisted of peroxidized linoleic acid and the respective spin trap dissolved in 20 mM phosphate buffer, pH 7.4, containing 1% acetonitrile. To this solution Fe^{2+}, dissolved in nitrogen-purged water, was added in order to start the formation of free radicals in a Fenton-type reaction, as recently tested with different DEPMPO [11,13] or EPPN [2] derivatives.

In Fig. 5, the radical adducts derived from linoleic acid hydroperoxide and the spin traps CPPyN-2 (Fig. 5a), CPPyN-3 (Fig. 5b), CPPyN-4 (Fig. 5c), and CPPN (Fig. 5d) generated in the anaerobic Fenton system are shown. The EPR spectra are typical of a partially immobilized carbon-centered radical adduct. The spectral parameters were obtained by computer simulation assuming the contribution of two different species to the observed EPR spectra (see also Table 5). In contrast to the two different stereoisomers of the α-hydroxyethyl radical adduct where the two nitrogen splittings were identical, the spectra of the LOOH-derived spin adducts could only be simulated using two different values for the nitrogen splitting. This makes the contribution of secondary, structurally different radicals likely, most probably stemming from degradation processes of the primary oxidation products. For comparison, the best fit for the contribution of a single species (assuming distorted lines and a high line width) is also given below in Table 5.

On the other hand, a contribution of spin adducts formed with the primary alkoxyl radical can be excluded since practically no change was observed even when concentrated solutions of the spin traps (around 100–150 mM) were used. In analogy to the EPPN series [2], also the PPyN derived spin traps form lipid radical adducts, which are considerably more stable (ca. 10–30 min) than those with DMPO or DEPMPO. Similar EPR spectra were obtained from the other spin traps tested (see Table 5).

4. Discussion

Twelve novel compounds derived from the spin traps PBN and EPPN were synthesized and fully characterized in this study. These substances form rather stable superoxide adducts ($t_{1/2}$ = 4–11 min), which are at least ten times more stable than the respective adducts with DMPO ($t_{1/2}$ = 45 s) [16] or PBN [3]. Only the superoxide adducts of some hydrophilic derivatives of EMPO ($t_{1/2}$ > 20 min [7]) or DEPMPO ($t_{1/2}$ = ca. 7–15 min [10,11,13]) are even more stable.

The half-lives of the superoxide adducts were determined using a first order exponential decay approximation (Pearson correlation coefficient $r^2 > 0.99$ except for CPPN ($r^2 = 0.97$) and CPPyN-2 ($r^2 = 0.98$)). Under the experimental conditions used a second order decay of the superoxide adducts was negligible. An important aspect which has to be considered is the fact that the observed spectral intensity not only depends on the half life of the spin adducts but also from the rate constant of the spin trapping reaction, the spectral line width and the total number of lines, and additional factors such as enzyme binding or the solubility (aggregate formation) of the spin trap. Preliminary tests, based on the spectral intensity of the respective superoxide spin adducts after 5 min, have shown that the performance of the PPyN compounds is between DMPO and DEPMPO, decreasing from the more hydrophilic to the more lipophilic compounds due to steric hindrance.

All novel compounds form also methoxyl and ethoxyl radical spin adducts. *n*-Octyloxyl adducts were detected with some of the tested compounds, e.g. with iPPPyN-2 and iPPPyN-3, which turned out to form the most stable alkoxyl radical adducts. Unfortunately, no alkoxyl radical spin adducts derived from peroxidized linoleic acid were found, even while employing higher concentrations of the spin trap. A severe limitation for the detection of such radicals is the fact that alkoxyl radicals undergo rapid β-scission with a rate constant of around 10^6, which efficiently competes with the spin trapping reaction. This applies especially as the maximum concentration of the different PPyN derivatives in aqueous solution did not exceed values about 100 mM. On the other hand, the spin

adducts formed from secondary carbon centered radicals, which are formed according to several pathways [17] in secondary reactions from $LOO^{\bullet}$ [18–23] and $LO^{\bullet}$, are very stable and were readily detected. The structure of the various secondary radical adduct could not be determined, but the oxygen in the primary alkoxyl radical formed from peroxidized linoleic acid is most likely situated in position 9 or 13. Depending on the reaction conditions, a variety of carbon-centered radicals can be formed from these primary radicals.

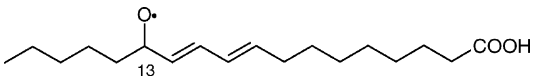

In conclusion, the four PPyN-3 derivatives can be recommended for the trapping of superoxide radicals, since the half-life of their superoxide adducts is 10 min or more. Hydroxyl radical adducts are not stable. The stability of alkoxyl radical adducts decreases with increasing chain length. Although the possibility to detect the primary alkoxyl radical formed during lipid peroxidation of fatty acids seems to be rather low, low-molecular weight secondary alkoxyl radicals should be detectable with iPPPyN-2 or iPPPyN-3, the alkoxyl radical adducts of which were stable for several minutes. In addition, all novel spin traps investigated can be recommended as possible alternatives to PBN for the detection of carbon-centered radicals. For this purpose, a homologous series of spin traps with increasing lipophilicity can readily be synthesized from commercially available compounds in two or three steps.

Acknowledgments

The authors wish to thank R. Stadtmüller for skilful technical assistance in synthesis, purification, and characterization of the spin traps. The present study was supported by the Austrian Fonds zur Förderung der wissenschaftlichen Forschung.

References

[1] Roubaud V, Lauricella R, Bouteiller JC, Tuccio B. *N*-2-(2-Ethoxycarbonyl-propyl)-α-phenylnitrone: an efficacious lipophilic spin trap for superoxide detection. Arch Biochem Biophys 2002;397:51–6.

[2] Stolze K, Udilova N, Rosenau T, Hofinger A, Nohl H. Spin trapping of superoxide, alkyl- and lipid-derived radicals with derivatives of the spin trap EPPN. Biochem Pharmacol 2003;66:1717–26.

[3] Janzen EG, Kotake Y, Hinton RD. Stabilities of hydroxyl radical spin adducts of PBN-type spin traps. Free Radical Biol Med 1992;12:169–73.

[4] Olive G, Mercier A, LeMoigne F, Rockenbauer A, Tordo P. 2-Ethoxycarbonyl-2-methyl-3,4-dihydro-2H-pyrrole-1-oxide: evaluation of the spin trapping properties. Free Radical Biol Med 2000;28:403–8.

[5] Zhang H, Joseph J, Vasquez-Vivar J, Karoui H, Nsanzumuhire C, Martásek P, et al. Detection of superoxide anion using an isotopically labeled nitrone spin trap: potential biological applications. FEBS Lett 2000;473:58–62.

[6] Stolze K, Udilova N, Nohl H. Spin adducts of superoxide, alkoxyl, and lipid-derived radicals with EMPO and its derivatives. Biol Chem 2002;383:813–20.

[7] Stolze K, Udilova N, Rosenau T, Hofinger A, Nohl H. Synthesis and characterization of EMPO-derived 5,5-disubstituted 1-pyrroline *N*-oxides as spin traps forming exceptionally stable superoxide spin adducts. Biol Chem 2003;384:493–500.

[8] Sankuratri N, Janzen EG. Synthesis and spin trapping chemistry of a novel bicyclic nitrone: 1,3,3-trimethyl-6-azabicyclo[3.2.1]oct-6-ene-*N*-oxide (Trazon). Tetrahedron Lett 1996;37:5313–6.

[9] Stolze K, Udilova N, Nohl H. ESR analysis of spin adducts of alkoxyl and lipid-derived radicals with the spin trap Trazon. Biochem Pharmacol 2002;63:1465–70.

[10] Fréjaville C, Karoui H, Tuccio B, Le Moigne F, Culcasi M, Pietri S, et al. 5-(Diethoxyphosphoryl)-5-methyl-1-pyrroline *N*-oxide: a new efficient phosphorylated nitrone for the in vitro and in vivo spin trapping of oxygen-centered radicals. J Med Chem 1995;38:258–65.

[11] Stolze K, Udilova N, Nohl H. Spin trapping of lipid radicals with DEPMPO-derived spin traps: detection of superoxide, alkyl and alkoxyl radicals in aqueous and lipid phase. Free Radical Biol Med 2000;29:1005–14.

[12] Dikalov SI, Mason RP. Spin trapping of polyunsaturated fatty acid-derived peroxyl radicals: reassignment to alkoxyl radical adducts. Free Radical Biol Med 2001;30:187–97.

[13] Stolze K, Udilova N, Nohl H. Lipid radicals: properties and detection by spin trapping. Acta Biochim Polonica 2000;47:923–30.

[14] O'Brien PJ. Intracellular mechanisms for the decomposition of a lipid peroxide. I. Decomposition of a lipid peroxide by metal ions, heme compounds, and nucleophiles. Can J Biochem 1969;47:485–92.

[15] Hawkes GE, Herwig K, Roberts JD. Nuclear magnetic resonance spectroscopy, use of ^{13}C spectra to establish configurations of oximes. J Org Chem 1974;39:1017–28.

[16] Buettner GR, Oberley LW. Considerations in the spin trapping of superoxide and hydroxyl radical in aqueous systems using 5,5-dimethyl-1-pyrroline-1-oxide. Biochem Biophys Res Commun 1978;83:69–74.

[17] Rota C, Barr DP, Martin MV, Guengerich FP, Tomasi A, Mason RP. Detection of free radicals produced from the reaction of cytochrome P-450 with linoleic acid hydroperoxide. Biochem J 1997;328:565–71.

[18] Van der Zee J, Barr DP, Mason RP. ESR spin trapping investigation of radical formation from the reaction between hematin and *tert*-butyl hydroperoxide. Free Radical Biol Med 1996;20:199–206.

[19] Akaike T, Sato K, Ijiri S, Miyamoto Y, Kohno M, Ando M, et al. Bactericidal activity of alkyl peroxyl radicals generated by heme-iron-catalyzed decomposition of organic peroxides. Arch Biochem Biophys 1992;294:55–63.

[20] Kalyanaraman B, Mottley C, Mason RP. A direct ESR and spin-trapping investigation of peroxyl free radical formation by hematin/hydroperoxide systems. J Biol Chem 1983;258:3855–8.

[21] Chamulitrat W, Takahashi N, Mason RP. Peroxyl, alkoxyl, and carbon-centered radical formation from organic hydroperoxides by chloroperoxidase. J Biol Chem 1989;264:7889–99.

[22] Davies MJ. Detection of peroxyl and alkoxyl radicals produced by reaction of hydroperoxides with heme-proteins by ESR spectroscopy. Biochim Biophys Acta 1988;964:28–35.

[23] Davies MJ. Detection of peroxyl and alkoxyl radicals produced by reaction of hydroperoxides with rat liver microsomal fractions. Biochem J 1989;257:603–6.